Toward TFlop Simulations of Supernovae

Konstantinos Kifonidis, Robert Buras, Andreas Marek, and Thomas Janka

Max Planck Institute for Astrophysics, Karl-Schwarzschild-Straße 1,
Postfach 1317, D-85741 Garching bei München, Germany,
kok@mpa-garching.mpg.de,
WWW home page: http://www.mpa-garching.mpg.de

Abstract We give an overview of the problems and the current status of (core collapse) supernova modelling, and report on our own recent progress, including the ongoing development of a code for multi-dimensional supernova simulations at TFlop speeds. In particular, we focus on the aspects of neutrino transport, and discuss the system of equations and the algorithm for its solution that are employed in this code. We also report first benchmark results from this code on an SGI Altix and a NEC SX-8.

1 Introduction

A star more massive than about 8 solar masses ends its live in a cataclysmic explosion, a supernova. Its quiescent evolution comes to an end, when the pressure in its inner layers is no longer able to balance the inward pull of gravity. Throughout its life, the star sustained this balance by generating energy through a sequence of nuclear fusion reactions, forming increasingly heavier elements in its core. However, when the core consists mainly of iron-group nuclei, central energy generation ceases. The fusion reactions producing iron-group nuclei relocate to the core's surface, and their "ashes" continuously increase the core's mass. Similar to a white dwarf, such a core is stabilized against gravity by the pressure of its degenerate gas of electrons. However, to remain stable, its mass must stay smaller than the Chandrasekhar limit. When the core grows larger than this limit, it collapses to a neutron star, and a huge amount ($\sim 10^{53}$ erg) of gravitational binding energy is set free. Most ($\sim 99\%$) of this energy is radiated away in neutrinos, but a small fraction is transferred to the outer stellar layers and drives the violent mass ejection which disrupts the star in a supernova.

Despite 40 years of research, the details of how this energy transfer happens and how the explosion is initiated are still not well understood. Observational evidence about the physical processes deep inside the collapsing star is sparse and almost exclusively indirect. The only direct observational access is via measurements of neutrinos or gravitational waves. To obtain insight into the events

in the core, one must therefore heavily rely on sophisticated numerical simulations. The enormous amount of computer power required for this purpose has led to the use of several, often questionable, approximations and numerous ambiguous results in the past. Fortunately, however, the development of numerical tools and computational resources has meanwhile advanced to a point, where it is becoming possible to perform multi-dimensional simulations with unprecedented accuracy. Therefore there is hope that the physical processes which are essential for the explosion can finally be unraveled.

An understanding of the explosion mechanism is required to answer many important questions of nuclear, gravitational, and astro-physics like the following:

- How do the explosion energy, the explosion timescale, and the mass of the compact remnant depend on the progenitor's mass? Is the explosion mechanism the same for all progenitors? For which stars are black holes left behind as compact remnants instead of neutron stars?
- What is the role of rotation during the explosion? How rapidly do newly formed neutron stars rotate? What are the implications for gamma-ray burst ("collapsar") models?
- How do neutron stars receive their natal kicks? Are they accelerated by asymmetric mass ejection and/or anisotropic neutrino emission?
- How much Fe-group elements and radioactive isotopes (e.g., ^{22}Na, ^{44}Ti, ^{56,57}Ni) are produced during the explosion, how are these elements mixed into the mantle and envelope of the exploding star, and what does their observation tell us about the explosion mechanism? Are supernovae responsible for the production of very massive chemical elements by the so-called "rapid neutron capture process" or r-process?
- What are the generic properties of the neutrino emission and of the gravitational wave signal that are produced during stellar core collapse and explosion? Up to which distances could these signals be measured with operating or planned detectors on earth and in space? And what can one learn about supernova dynamics from a future measurement of such signals in case of a Galactic supernova?

2 Numerical Models

2.1 History and Constraints

According to theory, a shock wave is launched at the moment of "core bounce" when the neutron star begins to emerge from the collapsing stellar iron core. There is general agreement, supported by all "modern" numerical simulations, that this shock is unable to propagate directly into the stellar mantle and envelope, because it looses too much energy in dissociating iron into free nucleons while it moves through the outer core. The "prompt" shock ultimately stalls. Thus the currently favored theoretical paradigm makes use of the fact that

a huge energy reservoir is present in the form of neutrinos, which are abundantly emitted from the hot, nascent neutron star. The absorption of electron neutrinos and antineutrinos by free nucleons in the post shock layer is thought to reenergize the shock, and lead to the supernova explosion.

Detailed *spherically symmetric* hydrodynamic models, which recently include a very accurate treatment of the time-dependent, multi-flavor, multi-frequency neutrino transport based on a numerical solution of the Boltzmann transport equation [1, 2, 3, 4], reveal that this "delayed, neutrino-driven mechanism" does not work as simply as originally envisioned. Although in principle able to trigger the explosion (e.g., [5], [6], [7]), neutrino energy transfer to the postshock matter turned out to be too weak. For inverting the infall of the stellar core and initiating powerful mass ejection, an increase of the efficiency of neutrino energy deposition is needed.

A number of physical phenomena have been pointed out that can enhance neutrino energy deposition behind the stalled supernova shock. They are all linked to the fact that the real world is multi-dimensional instead of spherically symmetric (or one-dimensional; 1D) as assumed in the work cited above:

(1) Convective instabilities in the neutrino-heated layer between the neutron star and the supernova shock develop to violent convective overturn [8]. This convective overturn is helpful for the explosion, mainly because (a) neutrino-heated matter rises and increases the pressure behind the shock, thus pushing the shock further out, and (b) cool matter is able to penetrate closer to the neutron star where it can absorb neutrino energy more efficiently. Both effects allow multi-dimensional models to explode easier than spherically symmetric ones [9, 10, 11].
(2) Recent work [12, 13, 14, 15] has demonstrated that the stalled supernova shock is also subject to a second non-radial instability which can grow to a dipolar, global deformation of the shock [15].
(3) Convective energy transport inside the nascent neutron star [16, 17, 18] might enhance the energy transport to the neutrinosphere and could thus boost the neutrino luminosities. This would in turn increase the neutrino-heating behind the shock.
(4) Rapid rotation of the collapsing stellar core and of the neutron star could lead to direction-dependent neutrino emission [19, 20] and thus anisotropic neutrino heating [21, 22]. Centrifugal forces, meridional circulation, pole-to-equator differences of the stellar structure, and magnetic fields could also have important consequences for the supernova evolution.

This list of multi-dimensional phenomena awaits more detailed exploration in multi-dimensional simulations. Until recently, such simulations have been performed with only a grossly simplified treatment of the involved microphysics, in particular of the neutrino transport and neutrino-matter interactions. At best, grey (i.e., single energy) flux-limited diffusion schemes were employed. All published successful simulations of supernova explosions by the convectively aided neutrino-heating mechanism in two [9, 10, 23, 24] and three dimensions [25, 26] used such a radical approximation of the neutrino transport.

Since, however, the role of the neutrinos is crucial for the problem, and because previous experience shows that the outcome of simulations is indeed very sensitive to the employed transport approximations, studies of the explosion mechanism require the best available description of the neutrino physics. This implies that one has to solve the Boltzmann transport equation for neutrinos.

2.2 Recent Calculations and the Need for TFlop Simulations

We have recently advanced to a new level of accuracy for supernova simulations by generalizing the VERTEX code, a Boltzmann solver for neutrino transport, from spherical symmetry [27] to multi-dimensional applications [28, 29, 30]. The corresponding mathematical model, and in particular our method for tackling the integro-differential transport problem in multi-dimensions, will be summarized in Sect. 3.

Results of a set of simulations with our code in 1D and 2D for progenitor stars with different masses have recently been published by [28], and with respect to the expected gravitational-wave signals from rotating and convective supernova cores by [31]. The recent progress in supernova modeling was summarized and set in perspective in a conference article by [29].

Our collection of simulations has helped us to identify a number of effects which have brought our two-dimensional models close to the threshold of explosion. This makes us optimistic that the solution of the long-standing problem of how massive stars explode may be in reach. In particular, we have recognized the following aspects as advantageous:

- Stellar rotation, even at a moderate level, supports the expansion of the stalled shock by centrifugal forces and instigates overturn motion in the neutrino-heated postshock matter by meridional circulation flows in addition to convective instabilities.
- Changing from the current "standard" and most widely used equation of state (EoS) for stellar core-collapse simulations [32] to alternative descriptions [33, 34], we found in 1D calculations that a higher incompressibility of the supranuclear phase yields a less dramatic and less rapid recession of the stalled shock after it has reached its maximum expansion [35]. This finding suggests that the EoS of [34] might lead to more favorable conditions for strong postshock convection, and thus more efficient neutrino heating, than current 2D simulations with the EoS of [32].
- Enlarging the two-dimensional grid from a 90° to a full 180° wedge, we indeed discovered global dipolar shock oscillations and a strong tendency for the growth of $l = 1$, 2 modes as observed also in previous models with a simplified treatment of neutrino transport [15]. The dominance of low-mode convection helped the expansion of the supernova shock in the 180°-simulation of an $11.2\,M_{\odot}$ star. In fact, the strongly deformed shock had expanded to a radius of more than 600 km at 226 ms post bounce with no tendency to return (Fig. 1). This model was on the way to an explosion, although probably a weak one, in contrast to simulations of the same star with a constrained

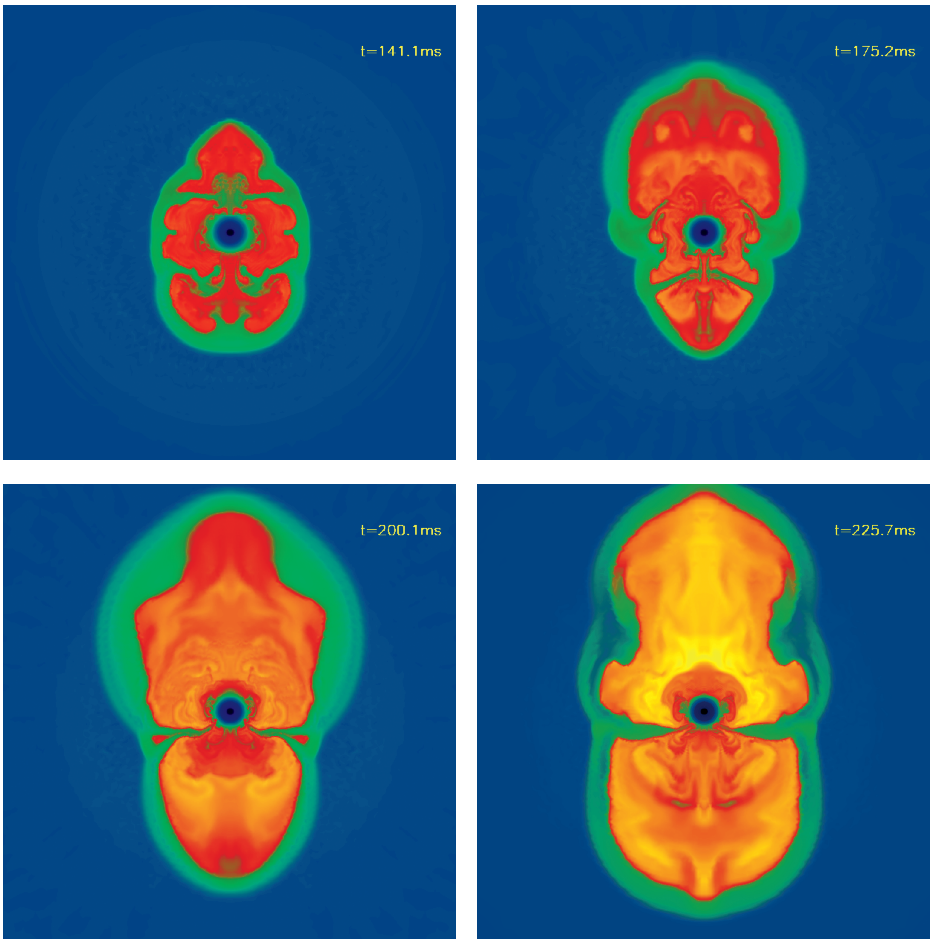

Fig. 1. Sequence of snapshots showing the large-scale convective overturn in the neutrino-heated postshock layer at four post-bounce times ($t_{\rm pb}$ = 141.1 ms, 175.2 ms, 200.1 ms, and 225.7 ms, from top left to bottom right) during the evolution of a (non-rotating) 11.2 $M_\odot$ progenitor star. The entropy is color coded with highest values being represented by red and yellow, and lowest values by blue and black. The dense neutron star is visible as a low-entropy circle at the center. A convective layer interior to the neutrinosphere cannot be visualized with the employed color scale because the entropy contrast there is small. Convection in this layer is driven by a negative gradient of the lepton number. The computation was performed with spherical coordinates, assuming axial symmetry, and employing the "ray-by-ray plus" variable Eddington factor technique for treating neutrino transport in multi-dimensional supernova simulations. Equatorial symmetry is broken on large scales soon after bounce, and low-mode convection begins to dominate the flow between the neutron star and the strongly deformed supernova shock. The model continues to develop a weak explosion. The scale of the plots is 1200 km in both directions.

90° wedge [29]. Unfortunately, calculating the first 226 ms of the evolution of this model already required about half a year of computer time on a 32 processor IBM p690, so that we were not able to continue the simulation to still later post-bounce times.

All these effects are potentially important, and some (or even all of them) may represent crucial ingredients for a successful supernova simulation. So far no multi-dimensional calculations have been performed, in which two or more of these items have been taken into account simultaneously, and thus their mutual interaction awaits to be investigated. It should also be kept in mind that our knowledge of supernova microphysics, and especially the EoS of neutron star matter, is still incomplete, which implies major uncertainties for supernova modeling. Unfortunately, the impact of different descriptions for this input physics has so far not been satisfactorily explored with respect to the neutrino-heating mechanism and the long-time behavior of the supernova shock, in particular in multi-dimensional models.

From this it is clear that rather extensive parameter studies using multi-dimensional simulations are required to identify the physical processes which are essential for the explosion. Since on a dedicated machine performing at a sustained speed of about 30 GFlops already a single 2D simulation has a turn-around time of more than half a year, these parameter studies are not possible without TFlop simulations.

3 The Mathematical Model

The non-linear system of partial differential equations which is solved in our code consists of the following components:

- The Euler equations of hydrodynamics, supplemented by advection equations for the electron fraction and the chemical composition of the fluid, and formulated in spherical coordinates;
- the Poisson equation for calculating the gravitational source terms which enter the Euler equations, including corrections for general relativistic effects;
- the Boltzmann transport equation which determines the (non-equilibrium) distribution function of the neutrinos;
- the emission, absorption, and scattering rates of neutrinos, which are required for the solution of the Boltzmann equation;
- the equation of state of the stellar fluid, which provides the closure relation between the variables entering the Euler equations, i.e. density, momentum, energy, electron fraction, composition, and pressure.

In what follows we will briefly summarize the neutrino transport algorithms. For a more complete description of the entire code we refer the reader to [28], [30], and the references therein.

3.1 "Ray-by-ray plus" Variable Eddington Factor Solution of the Neutrino Transport Problem

The crucial quantity required to determine the source terms for the energy, momentum, and electron fraction of the fluid owing to its interaction with the neutrinos is the neutrino distribution function in phase space, $f(r, \vartheta, \phi, \epsilon, \Theta, \Phi, t)$. Equivalently, the neutrino intensity $I = c/(2\pi\hbar c)^3 \cdot \epsilon^3 f$ may be used. Both are seven-dimensional functions, as they describe, at every point in space (r, ϑ, ϕ), the distribution of neutrinos propagating with energy ϵ into the direction (Θ, Φ) at time t (Fig. 2).

The evolution of I (or f) in time is governed by the Boltzmann equation, and solving this equation is, in general, a six-dimensional problem (since time is usually not counted as a separate dimension). A solution of this equation by direct discretization (using an S_N scheme) would require computational resources in the PetaFlop range. Although there are attempts by at least one group in the United States to follow such an approach, we feel that, with the currently available computational resources, it is mandatory to reduce the dimensionality of the problem.

Actually this should be possible, since the source terms entering the hydrodynamic equations are *integrals* of I over momentum space (i.e. over ϵ, Θ, and Φ), and thus only a fraction of the information contained in I is truly required to compute the dynamics of the flow. It makes therefore sense to consider angular moments of I, and to solve evolution equations for these moments, instead of dealing with the Boltzmann equation directly. The 0th to 3rd order moments are defined as

$$J, \boldsymbol{H}, \mathbf{K}, \mathbf{L}, \ldots (r, \vartheta, \phi, \epsilon, t) = \frac{1}{4\pi} \int I(r, \vartheta, \phi, \epsilon, \Theta, \Phi, t)\, \boldsymbol{n}^{0,1,2,3,\cdots}\, \mathrm{d}\Omega \qquad (1)$$

where $\mathrm{d}\Omega = \sin\Theta\, \mathrm{d}\Theta\, \mathrm{d}\Phi$, $\boldsymbol{n} = (\sin\Theta\cos\Phi, \sin\Theta\sin\Phi, \cos\Theta)$, and exponentiation represents repeated application of the dyadic product. Note that the moments are *tensors* of the required rank.

This leaves us with a four-dimensional problem. So far no approximations have been made. In order to reduce the size of the problem even further, one

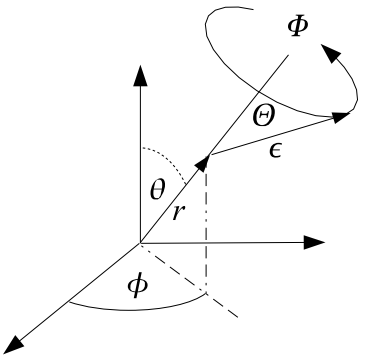

Fig. 2. Illustration of the phase space coordinates (see the main text).

needs to resort to assumptions on its symmetry. At this point, one usually employs azimuthal symmetry for the stellar matter distribution, i.e. any dependence on the azimuth angle ϕ is ignored, which implies that the hydrodynamics of the problem can be treated in two dimensions. It also implies $I(r,\vartheta,\epsilon,\Theta,\Phi) = I(r,\vartheta,\epsilon,\Theta,-\Phi)$. If, in addition, it is assumed that I is even independent of Φ, then each of the angular moments of I becomes a *scalar*, which depends on two spatial dimensions, and one dimension in momentum space: $J,H,K,L = J,H,K,L(r,\vartheta,\epsilon,t)$. Thus we have reduced the problem to three dimensions in total.

The System of Equations

With the aforementioned assumptions it can be shown [30], that in order to compute the source terms for the energy and electron fraction of the fluid, the following two transport equations need to be solved:

$$\left(\frac{1}{c}\frac{\partial}{\partial t}+\beta_r\frac{\partial}{\partial r}+\frac{\boldsymbol{\beta_\vartheta}}{\boldsymbol{r}}\frac{\boldsymbol{\partial}}{\boldsymbol{\partial\vartheta}}\right)J+J\left(\frac{1}{r^2}\frac{\partial(r^2\beta_r)}{\partial r}+\frac{\mathbf{1}}{\boldsymbol{r}\sin\boldsymbol{\vartheta}}\frac{\boldsymbol{\partial}(\sin\boldsymbol{\vartheta}\boldsymbol{\beta_\vartheta})}{\boldsymbol{\partial\vartheta}}\right)$$
$$+\frac{1}{r^2}\frac{\partial(r^2H)}{\partial r}+\frac{\beta_r}{c}\frac{\partial H}{\partial t}-\frac{\partial}{\partial\epsilon}\left\{\frac{\epsilon}{c}\frac{\partial\beta_r}{\partial t}H\right\}-\frac{\partial}{\partial\epsilon}\left\{\epsilon J\left(\frac{\beta_r}{r}+\frac{\mathbf{1}}{\boldsymbol{2r}\sin\boldsymbol{\vartheta}}\frac{\boldsymbol{\partial}(\sin\boldsymbol{\vartheta}\boldsymbol{\beta_\vartheta})}{\boldsymbol{\partial\vartheta}}\right)\right\}$$
$$-\frac{\partial}{\partial\epsilon}\left\{\epsilon K\left(\frac{\partial\beta_r}{\partial r}-\frac{\beta_r}{r}-\frac{\mathbf{1}}{\boldsymbol{2r}\sin\boldsymbol{\vartheta}}\frac{\boldsymbol{\partial}(\sin\boldsymbol{\vartheta}\boldsymbol{\beta_\vartheta})}{\boldsymbol{\partial\vartheta}}\right)\right\}+J\left(\frac{\beta_r}{r}+\frac{\mathbf{1}}{\boldsymbol{2r}\sin\boldsymbol{\vartheta}}\frac{\boldsymbol{\partial}(\sin\boldsymbol{\vartheta}\boldsymbol{\beta_\vartheta})}{\boldsymbol{\partial\vartheta}}\right)$$
$$+K\left(\frac{\partial\beta_r}{\partial r}-\frac{\beta_r}{r}-\frac{\mathbf{1}}{\boldsymbol{2r}\sin\boldsymbol{\vartheta}}\frac{\boldsymbol{\partial}(\sin\boldsymbol{\vartheta}\boldsymbol{\beta_\vartheta})}{\boldsymbol{\partial\vartheta}}\right)+\frac{2}{c}\frac{\partial\beta_r}{\partial t}H=C^{(0)}, \quad (2)$$

$$\left(\frac{1}{c}\frac{\partial}{\partial t}+\beta_r\frac{\partial}{\partial r}+\frac{\boldsymbol{\beta_\vartheta}}{\boldsymbol{r}}\frac{\boldsymbol{\partial}}{\boldsymbol{\partial\vartheta}}\right)H+H\left(\frac{1}{r^2}\frac{\partial(r^2\beta_r)}{\partial r}+\frac{\mathbf{1}}{\boldsymbol{r}\sin\boldsymbol{\vartheta}}\frac{\boldsymbol{\partial}(\sin\boldsymbol{\vartheta}\boldsymbol{\beta_\vartheta})}{\boldsymbol{\partial\vartheta}}\right)$$
$$+\frac{\partial K}{\partial r}+\frac{3K-J}{r}+H\left(\frac{\partial\beta_r}{\partial r}\right)+\frac{\beta_r}{c}\frac{\partial K}{\partial t}-\frac{\partial}{\partial\epsilon}\left\{\frac{\epsilon}{c}\frac{\partial\beta_r}{\partial t}K\right\}$$
$$-\frac{\partial}{\partial\epsilon}\left\{\epsilon L\left(\frac{\partial\beta_r}{\partial r}-\frac{\beta_r}{r}-\frac{\mathbf{1}}{\boldsymbol{2r}\sin\boldsymbol{\vartheta}}\frac{\boldsymbol{\partial}(\sin\boldsymbol{\vartheta}\boldsymbol{\beta_\vartheta})}{\boldsymbol{\partial\vartheta}}\right)\right\}$$
$$-\frac{\partial}{\partial\epsilon}\left\{\epsilon H\left(\frac{\beta_r}{r}+\frac{\mathbf{1}}{\boldsymbol{2r}\sin\boldsymbol{\vartheta}}\frac{\boldsymbol{\partial}(\sin\boldsymbol{\vartheta}\boldsymbol{\beta_\vartheta})}{\boldsymbol{\partial\vartheta}}\right)\right\}+\frac{1}{c}\frac{\partial\beta_r}{\partial t}(J+K)=C^{(1)}. \quad (3)$$

These are evolution equations for the neutrino energy density, J, and the neutrino flux, H, and follow from the zeroth and first moment equations of the comoving frame (Boltzmann) transport equation in the Newtonian, $\mathcal{O}(v/c)$ approximation. The quantities $C^{(0)}(J,H)$ and $C^{(1)}(J,H)$ are source terms that result from the collision term of the Boltzmann equation, while $\beta_r = v_r/c$ and $\beta_\vartheta = v_\vartheta/c$, where v_r and v_ϑ are the components of the hydrodynamic velocity, and c is the speed of light. The functional dependences $\beta_r = \beta_r(r,\vartheta,t)$, $J = J(r,\vartheta,\epsilon,t)$, etc. are suppressed in the notation. This system includes four unknown moments (J,H,K,L) but only two equations, and thus needs to be

supplemented by two more relations. This is done by substituting $K = f_K \cdot J$ and $L = f_L \cdot J$, where f_K and f_L are the variable Eddington factors, which for the moment may be regarded as being known, but in general must be determined from a separate system of equations (see below).

A finite volume discretization of Eqs. (2–3) is sufficient to guarantee exact conservation of the total neutrino energy. However, and as described in detail in [27], it is not sufficient to guarantee also exact conservation of the neutrino number. To achieve this, we discretize and solve a set of two additional equations. With $\mathcal{J} = J/\epsilon$, $\mathcal{H} = H/\epsilon$, $\mathcal{K} = K/\epsilon$, and $\mathcal{L} = L/\epsilon$, this set of equations reads

$$\begin{aligned}
&\left(\frac{1}{c}\frac{\partial}{\partial t} + \beta_r\frac{\partial}{\partial r} + \frac{\boldsymbol{\beta_\vartheta}}{\boldsymbol{r}}\frac{\boldsymbol{\partial}}{\boldsymbol{\partial\vartheta}}\right)\mathcal{J} + \mathcal{J}\left(\frac{1}{r^2}\frac{\partial(r^2\beta_r)}{\partial r} + \frac{\mathbf{1}}{\boldsymbol{r\sin\vartheta}}\frac{\boldsymbol{\partial(\sin\vartheta\beta_\vartheta)}}{\boldsymbol{\partial\vartheta}}\right)\\
&+\frac{1}{r^2}\frac{\partial(r^2\mathcal{H})}{\partial r} + \frac{\beta_r}{c}\frac{\partial\mathcal{H}}{\partial t} - \frac{\partial}{\partial\epsilon}\left\{\frac{\epsilon}{c}\frac{\partial\beta_r}{\partial t}\mathcal{H}\right\} - \frac{\partial}{\partial\epsilon}\left\{\epsilon\mathcal{J}\left(\frac{\beta_r}{r} + \frac{\mathbf{1}}{\boldsymbol{2r\sin\vartheta}}\frac{\boldsymbol{\partial(\sin\vartheta\beta_\vartheta)}}{\boldsymbol{\partial\vartheta}}\right)\right\}\\
&- \frac{\partial}{\partial\epsilon}\left\{\epsilon\mathcal{K}\left(\frac{\partial\beta_r}{\partial r} - \frac{\beta_r}{r} - \frac{\mathbf{1}}{\boldsymbol{2r\sin\vartheta}}\frac{\boldsymbol{\partial(\sin\vartheta\beta_\vartheta)}}{\boldsymbol{\partial\vartheta}}\right)\right\} + \frac{1}{c}\frac{\partial\beta_r}{\partial t}\mathcal{H} = \mathcal{C}^{(0)}, \quad (4)
\end{aligned}$$

$$\begin{aligned}
&\left(\frac{1}{c}\frac{\partial}{\partial t} + \beta_r\frac{\partial}{\partial r} + \frac{\boldsymbol{\beta_\vartheta}}{\boldsymbol{r}}\frac{\boldsymbol{\partial}}{\boldsymbol{\partial\vartheta}}\right)\mathcal{H} + \mathcal{H}\left(\frac{1}{r^2}\frac{\partial(r^2\beta_r)}{\partial r} + \frac{\mathbf{1}}{\boldsymbol{r\sin\vartheta}}\frac{\boldsymbol{\partial(\sin\vartheta\beta_\vartheta)}}{\boldsymbol{\partial\vartheta}}\right)\\
&+ \frac{\partial\mathcal{K}}{\partial r} + \frac{3\mathcal{K} - \mathcal{J}}{r} + \mathcal{H}\left(\frac{\partial\beta_r}{\partial r}\right) + \frac{\beta_r}{c}\frac{\partial\mathcal{K}}{\partial t} - \frac{\partial}{\partial\epsilon}\left\{\frac{\epsilon}{c}\frac{\partial\beta_r}{\partial t}\mathcal{K}\right\}\\
&- \frac{\partial}{\partial\epsilon}\left\{\epsilon\mathcal{L}\left(\frac{\partial\beta_r}{\partial r} - \frac{\beta_r}{r} - \frac{\mathbf{1}}{\boldsymbol{2r\sin\vartheta}}\frac{\boldsymbol{\partial(\sin\vartheta\beta_\vartheta)}}{\boldsymbol{\partial\vartheta}}\right)\right\}\\
&- \frac{\partial}{\partial\epsilon}\left\{\epsilon\mathcal{H}\left(\frac{\beta_r}{r} + \frac{\mathbf{1}}{\boldsymbol{2r\sin\vartheta}}\frac{\boldsymbol{\partial(\sin\vartheta\beta_\vartheta)}}{\boldsymbol{\partial\vartheta}}\right)\right\} - \mathcal{L}\left(\frac{\partial\beta_r}{\partial r} - \frac{\beta_r}{r} - \frac{\mathbf{1}}{\boldsymbol{2r\sin\vartheta}}\frac{\boldsymbol{\partial(\sin\vartheta\beta_\vartheta)}}{\boldsymbol{\partial\vartheta}}\right)\\
&- \mathcal{H}\left(\frac{\beta_r}{r} + \frac{\mathbf{1}}{\boldsymbol{2r\sin\vartheta}}\frac{\boldsymbol{\partial(\sin\vartheta\beta_\vartheta)}}{\boldsymbol{\partial\vartheta}}\right) + \frac{1}{c}\frac{\partial\beta_r}{\partial t}\mathcal{J} = \mathcal{C}^{(1)}. \quad (5)
\end{aligned}$$

The moment Eqs. (2–5) are very similar to the $\mathcal{O}(v/c)$ equations in spherical symmetry which were solved in the 1D simulations of [27] (see Eqs. (7), (8), (30), and (31) of the latter work). This similarity has allowed us to reuse a good fraction of the one-dimensional version of VERTEX, for coding the multi-dimensional algorithm. The additional terms necessary for this purpose have been set in boldface above.

Finally, the changes of the energy, e, and electron fraction, Y_e, required for the hydrodynamics are given by the following two equations

$$\frac{\mathrm{d}e}{\mathrm{d}t} = -\frac{4\pi}{\rho}\int_0^\infty \mathrm{d}\epsilon \sum_{\nu\in(\nu_\mathrm{e},\bar{\nu}_\mathrm{e},\dots)} C_\nu^{(0)}\left(J(\epsilon), H(\epsilon)\right), \quad (6)$$

$$\frac{\mathrm{d}Y_\mathrm{e}}{\mathrm{d}t} = -\frac{4\pi\, m_\mathrm{B}}{\rho}\int_0^\infty \mathrm{d}\epsilon \left(\mathcal{C}_{\nu_\mathrm{e}}^{(0)}\left(\mathcal{J}(\epsilon), \mathcal{H}(\epsilon)\right) - \mathcal{C}_{\bar{\nu}_\mathrm{e}}^{(0)}\left(\mathcal{J}(\epsilon), \mathcal{H}(\epsilon)\right)\right) \quad (7)$$

(for the momentum source terms due to neutrinos see [30]). Here m_B is the baryon mass, and the sum in Eq. (6) runs over all neutrino types. The full system

consisting of Eqs. (2–7) is stiff, and thus requires an appropriate discretization scheme for its stable solution.

Method of Solution

In order to discretize Eqs. (2–7), the spatial domain $[0, r_{\max}] \times [\vartheta_{\min}, \vartheta_{\max}]$ is covered by N_r radial, and N_ϑ angular zones, where $\vartheta_{\min} = 0$ and $\vartheta_{\max} = \pi$ correspond to the north and south poles, respectively, of the spherical grid. (In general, we allow for grids with different radial resolutions in the neutrino transport and hydrodynamic parts of the code. The number of radial zones for the hydrodynamics will be denoted by $N_r^{\rm hyd}$.) The number of bins used in energy space is N_ϵ and the number of neutrino types taken into account is N_ν.

The equations are solved in two operator-split steps corresponding to a lateral and a radial sweep.

In the first step, we treat the boldface terms in the respectively first lines of Eqs. (2–5), which describe the lateral advection of the neutrinos with the stellar fluid, and thus couple the angular moments of the neutrino distribution of neighbouring angular zones. For this purpose we consider the equation

$$\frac{1}{c}\frac{\partial \Xi}{\partial t} + \frac{1}{r \sin\vartheta}\frac{\partial(\sin\vartheta\, \beta_\vartheta\, \Xi)}{\partial \vartheta} = 0\,, \tag{8}$$

where Ξ represents one of the moments J, H, $\mathcal{J}$, or $\mathcal{H}$. Although it has been suppressed in the above notation, an equation of this form has to be solved for each radius, for each energy bin, and for each type of neutrino. An explicit upwind scheme is used for this purpose.

In the second step, the radial sweep is performed. Several points need to be noted here:

- terms in boldface not yet taken into account in the lateral sweep, need to be included into the discretization scheme of the radial sweep. This can be done in a straightforward way since these remaining terms do not include ϑ-derivatives of the transport variables (J, H) or $(\mathcal{J}, \mathcal{H})$. They only include ϑ-derivatives of the hydrodynamic velocity v_ϑ, which is a *constant* scalar field for the transport problem.
- the right hand sides (source terms) of the equations and the coupling in energy space have to be accounted for. The coupling in energy is non-local, since the source terms of Eqs. (2–5) stem from the Boltzmann equation, which is an integro-differential equation and couples all the energy bins
- the discretization scheme for the radial sweep is *implicit* in time. Explicit schemes would require very small time steps to cope with the stiffness of the source terms in the optically thick regime, and the small CFL time step dictated by neutrino propagation with the speed of light in the optically thin regime. Still, even with an implicit scheme $\gtrsim 10^5$ time steps are required per simulation. This makes the calculations expensive.

Once the equations for the radial sweep have been discretized in radius and energy, the resulting solver is applied ray-by-ray for each angle ϑ and for each

type of neutrino, i.e. for constant ϑ, N_ν two-dimensional problems need to be solved.

The discretization itself is done using a second order accurate scheme with backward differencing in time according to [27]. This leads to a non-linear system of algebraic equations, which is solved by Newton-Raphson iteration with explicit construction and inversion of the corresponding Jacobian matrix.

Inversion of the Jacobians

The Jacobians resulting from the radial sweep are block-pentadiagonal matrices with $2 \times N_r + 1$ rows of blocks. The blocks themselves are dense, because of the non-local coupling in energy. For the transport of electron neutrinos and antineutrinos, the blocks are of dimension $(2 \times N_\epsilon + 2)^2$, or $(4 \times N_\epsilon + 2)^2$, depending, respectively, on whether only Eqs. (2), (3), (6), and (7) or the full system consisting of Eqs. (2–7) is solved (see below).

Three alternative direct methods are currently implemented for solving the resulting linear systems. The first is a Block-Thomas solver which uses optimized routines from the BLAS and LAPACK libraries to perform the necessary LU decompositions and backsubstitutions of the dense blocks. In this case vectorization is used within BLAS, i.e. within the operations on blocks, and the achievable vector length is determined by the block size.

The second is a block cyclic reduction solver which also uses BLAS and LAPACK for block operations.

The third is a block cyclic reduction solver that is vectorized along the Jacobians' diagonals (i.e. along the radius, r) in order to obtain longer vector lengths. This might be of advantage in case a simulation needs to be set up with a small resolution in energy space, resulting in a correspondingly small size of the single blocks.

Variable Eddington Factors

To solve Eqs. (2–7), we need the variable Eddington factors $f_K = K/J$ and $f_L = L/J$. These closure relations are obtained from the solution of a simplified ("model") Boltzmann equation. The integro-differential character of this equation is tackled by expressing the angular integrals in the interaction kernels of its right-hand side, with the moments J and H, for which estimates are obtained from a solution of the system of moment equations (2–3), (6) and (7). With the right-hand side known, the model Boltzmann equation is solved by means of the so-called tangent ray method (see [36], and [27] for details), and the entire procedure is iterated until convergence of the Eddington factors is achieved (cf. Fig. 3).

Note that this apparently involved procedure is computationally efficient, because the Eddington factors are geometrical quantities, which vary only slowly, and thus can be computed relatively cheaply using only a "model" transport equation. Note also that only the system of Eqs. (2–3), (6) and (7), and not the full system Eqs. (2–7), is used in the iteration. This allows us to save computer

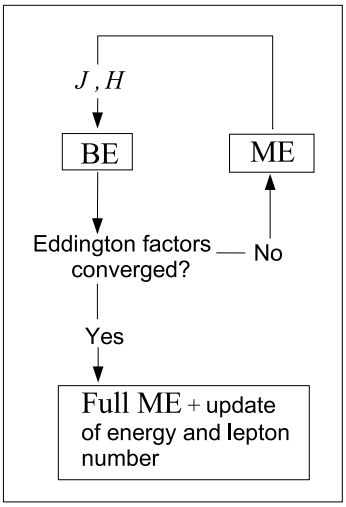

Fig. 3. Illustration of the iteration procedure for calculating the variable Eddington factors. The boxes labeled ME and BE represent the solution algorithms for the moment equations, and the "model" Boltzmann equation, respectively (see the text for details).

time. Once the Eddington factors are known, the complete system Eqs. (2–7), enforcing conservation of energy and neutrino number, is solved once, in order to update the energy and electron fraction (lepton number) of the fluid.

In contrast to previous work [27, 30], our latest code version takes into account that the Eddington factors are functions of radius and angle, $f_K = f_K(r, \vartheta, t)$ and $f_L = f_L(r, \vartheta, t)$, and thus the iteration procedure shown in Fig. 3 is applied on each ray, i.e. for each ϑ.

4 Implementation and First Benchmarks

The VERTEX routines, that have been described above, have been coupled to the hydrodynamics code PROMETHEUS, to obtain the full supernova code PROMETHEUS/VERTEX. In a typical low-resolution supernova simulation, like the one shown in Fig. 1 and corresponding to setup "S" of Table 1, the VERTEX transport routines typically account for 99.5%, and the hydrodynamics for about 0.5% of the entire execution time. The ratio of computing times is expected to tilt even further towards the transport side when the larger setups in Table 1 are investigated (especially the one with 34 energy bins), since a good fraction of the total time is spent in inverting the Jacobians. It is thus imperative to achieve good parallel scalability, and good vector performance of the neutrino transport routines.

Two parallel code versions of PROMETHEUS/VERTEX are currently available. The first uses a two-level hierarchical parallel programming model that exploits instruction level parallelism through vectorization and shared memory parallelism by macrotasking with OpenMP directives. The second code version is similar to the first one, but adds to these two levels also distributed memory parallelism using message passing with MPI.

The nature of the employed algorithms naturally lends itself to a hierarchical programming model because of the fact that directional (operator) splitting is

used in both the hydrodynamic as well as the neutrino transport parts of the code. Thus one needs to perform logically independent, lower-dimensional sub-integrations in order to solve a multi-dimensional problem. For instance, the $N_\vartheta \times N_\nu$ and $N_r \times N_\epsilon \times N_\nu$ integrations resulting within the r and ϑ transport sweeps, respectively, can be performed in parallel with coarse granularity. The routines used to perform the lower-dimensional sub-integrations are then completely vectorized.

Figure 4 shows scaling results of the OpenMP code version on an SGI Altix 3700 Bx2 (using Itanium2 CPUs with 6 MB L3 caches). The measurements are for the S and M setups of Table 1. The Thomas solver has been used to invert the Jacobians. The speedup is initially superlinear, while on 64 processors it is close to 60, demonstrating the efficiency of the employed parallelization strategy. Note that static scheduling of the parallel sub-integrations has been applied, because the Altix is a ccNUMA machine which requires a minimization of remote memory references to achieve good scaling. Dynamic scheduling would not guarantee this, although it would actually be preferable from the algorithmic point of view, to obtain optimal load balancing.

Table 1. Some typical setups with different resolutions.

Setup	N_r^{hyd}	N_r	N_ϑ	N_ϵ	N_ν
XS	400	234	32	17	3
S	400	234	126	17	3
M	400	234	256	17	3
L	800	468	512	17	3
XL	800	468	512	34	3

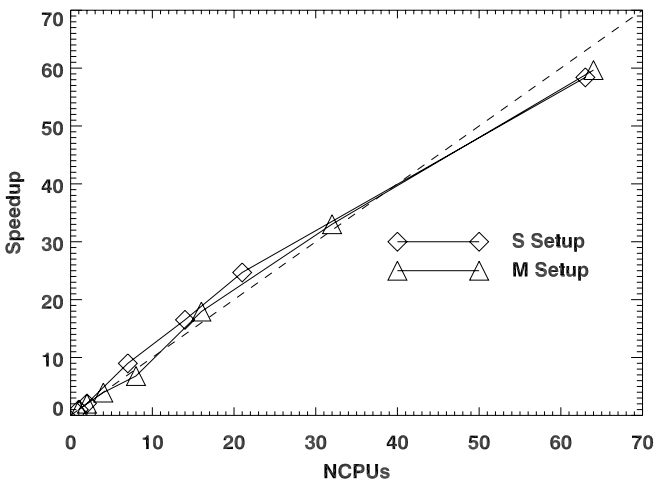

Fig. 4. Scaling of PROMETHEUS/VERTEX on the SGI Altix 3700 Bx2.

Table 2. First measurements of the OpenMP code version on (a single compute node of) an NEC SX-6+ and an NEC SX-8. Times are given in seconds.

Measurements on the SX-6+				
Setup	NCPUs	(avg.) wallclock time/cycle	Speedup	MFLOPs/sec
XS	1	211.25	1.00	2708
XS	4	59.67	3.54	9339
XS	8	34.42	6.14	15844
Measurements on the SX-8				
Setup	NCPUs	(avg.) wallclock time/cycle	Speedup	MFLOPs/sec
XS	1	139.08	1.00	4119
XS	4	39.17	3.43	14181
XS	8	22.75	6.11	23773
S	1	457.71	1.00	4203
S	4	133.43	3.43	13870
S	8	78.43	5.83	22838
M	1	926.14	1.00	4203
M	4	268.29	3.45	13937
M	8	159.14	5.82	22759

The behaviour of the same code on the (cacheless) NEC SX-6+ and NEC SX-8 is shown in Table 2. One can note that (for the same number of processors) the measured speedups are noticeably smaller than on the SGI. Moreover the larger problem setups (with more angular zones) scale *worse* than the smaller ones, indicating that a load imbalance is present. On these "flat memory" machines with their very fast processors a good load balance is apparently much more crucial for obtaining good scalability, and dynamic scheduling of the sub-integrations might have been the better choice. Table 2 also lists the FLOP rates for the entire code (including I/O, initializations and other overhead). The vector performance achieved with the listed setups on a single CPU of the NEC machines is between 26% and 30% of the peak performance. Given that in any case only 17 energy bins have been used in these tests, and that therefore the average vector length achieved in the calculations was only about 110 (on an architecture where vector lengths $\gtrsim 256$ are considered optimal), this computational rate appears quite satisfactory. Improvements are still possible, though, and optimization of the code on NEC machines is in progress.

Acknowledgements

Support from the SFB 375 "Astroparticle Physics" of the Deutsche Forschungsgemeinschaft, and computer time at the HLRS and the Rechenzentrum Garching

are acknowledged. We also thank M. Galle and R. Fischer for performing the benchmarks on the NEC machines.

References

1. Rampp, M., Janka, H.T.: Spherically Symmetric Simulation with Boltzmann Neutrino Transport of Core Collapse and Postbounce Evolution of a 15 $M_\odot$ Star. Astrophys. J. **539** (2000) L33–L36
2. Mezzacappa, A., Liebendörfer, M., Messer, O.E., Hix, W.R., Thielemann, F., Bruenn, S.W.: Simulation of the Spherically Symmetric Stellar Core Collapse, Bounce, and Postbounce Evolution of a Star of 13 Solar Masses with Boltzmann Neutrino Transport, and Its Implications for the Supernova Mechanism. Phys. Rev. Letters **86** (2001) 1935–1938
3. Liebendörfer, M., Mezzacappa, A., Thielemann, F., Messer, O.E., Hix, W.R., Bruenn, S.W.: Probing the gravitational well: No supernova explosion in spherical symmetry with general relativistic Boltzmann neutrino transport. Phys. Rev. D **63** (2001) 103004–+
4. Thompson, T.A., Burrows, A., Pinto, P.A.: Shock Breakout in Core-Collapse Supernovae and Its Neutrino Signature. Astrophys. J. **592** (2003) 434–456
5. Bethe, H.A.: Supernova mechanisms. Reviews of Modern Physics **62** (1990) 801–866
6. Burrows, A., Goshy, J.: A Theory of Supernova Explosions. Astrophys. J. **416** (1993) L75
7. Janka, H.T.: Conditions for shock revival by neutrino heating in core-collapse supernovae. Astron. Astrophys. **368** (2001) 527–560
8. Herant, M., Benz, W., Colgate, S.: Postcollapse hydrodynamics of SN 1987A – Two-dimensional simulations of the early evolution. Astrophys. J. **395** (1992) 642–653
9. Herant, M., Benz, W., Hix, W.R., Fryer, C.L., Colgate, S.A.: Inside the supernova: A powerful convective engine. Astrophys. J. **435** (1994) 339
10. Burrows, A., Hayes, J., Fryxell, B.A.: On the nature of core-collapse supernova explosions. Astrophys. J. **450** (1995) 830
11. Janka, H.T., Müller, E.: Neutrino heating, convection, and the mechanism of Type-II supernova explosions. Astron. Astrophys. **306** (1996) 167–+
12. Thompson, C.: Accretional Heating of Asymmetric Supernova Cores. Astrophys. J. **534** (2000) 915–933
13. Foglizzo, T.: Non-radial instabilities of isothermal Bondi accretion with a shock: Vortical-acoustic cycle vs. post-shock acceleration. Astron. Astrophys. **392** (2002) 353–368
14. Blondin, J.M., Mezzacappa, A., DeMarino, C.: Stability of Standing Accretion Shocks, with an Eye toward Core-Collapse Supernovae. Astrophys. J. **584** (2003) 971–980
15. Scheck, L., Plewa, T., Janka, H.T., Kifonidis, K., Müller, E.: Pulsar Recoil by Large-Scale Anisotropies in Supernova Explosions. Phys. Rev. Letters **92** (2004) 011103–+
16. Keil, W., Janka, H.T., Mueller, E.: Ledoux Convection in Protoneutron Stars – A Clue to Supernova Nucleosynthesis? Astrophys. J. **473** (1996) L111
17. Burrows, A., Lattimer, J.M.: The birth of neutron stars. Astrophys. J. **307** (1986) 178–196

18. Pons, J.A., Reddy, S., Prakash, M., Lattimer, J.M., Miralles, J.A.: Evolution of Proto-Neutron Stars. Astrophys. J. **513** (1999) 780–804
19. Janka, H.T., Mönchmeyer, R.: Anisotropic neutrino emission from rotating protoneutron stars. Astron. Astrophys. **209** (1989) L5–L8
20. Janka, H.T., Mönchmeyer, R.: Hydrostatic post bounce configurations of collapsed rotating iron cores – Neutrino emission. Astron. Astrophys. **226** (1989) 69–87
21. Shimizu, T.M., Ebisuzaki, T., Sato, K., Yamada, S.: Effect of Anisotropic Neutrino Radiation on Supernova Explosion Energy. Astrophys. J. **552** (2001) 756–781
22. Kotake, K., Yamada, S., Sato, K.: Anisotropic Neutrino Radiation in Rotational Core Collapse. Astrophys. J. **595** (2003) 304–316
23. Fryer, C.L.: Mass Limits For Black Hole Formation. Astrophys. J. **522** (1999) 413–418
24. Fryer, C.L., Heger, A.: Core-Collapse Simulations of Rotating Stars. Astrophys. J. **541** (2000) 1033–1050
25. Fryer, C.L., Warren, M.S.: Modeling Core-Collapse Supernovae in Three Dimensions. Astrophys. J. **574** (2002) L65–L68
26. Fryer, C.L., Warren, M.S.: The Collapse of Rotating Massive Stars in Three Dimensions. Astrophys. J. **601** (2004) 391–404
27. Rampp, M., Janka, H.T.: Radiation hydrodynamics with neutrinos. Variable Eddington factor method for core-collapse supernova simulations. Astron. Astrophys. **396** (2002) 361–392
28. Buras, R., Rampp, M., Janka, H.T., Kifonidis, K.: Improved Models of Stellar Core Collapse and Still No Explosions: What Is Missing? Phys. Rev. Letters **90** (2003) 241101–+
29. Janka, H.T., Buras, R., Kifonidis, K., Marek, A., Rampp, M.: Core-Collapse Supernovae at the Threshold. In Marcaide, J.M., Weiler, K.W., eds.: Supernovae, Procs. of the IAU Coll. 192, Berlin, Springer (2004)
30. Buras, R., Rampp, M., Janka, H.T., Kifonidis, K., Takahashi, K., Horowitz, C.J.: Two-dimensional hydrodynamic core collapse supernova simulations with spectral neutrino transport. Astron. Astrophys. (2006), to appear
31. Müller, E., Rampp, M., Buras, R., Janka, H.T., Shoemaker, D.H.: Toward Gravitational Wave Signals from Realistic Core-Collapse Supernova Models. Astrophys. J. **603** (2004) 221–230
32. Lattimer, J.M., Swesty, F.D.: A generalized equation of state for hot, dense manner. Nuclear Physics A **535** (1991) 331–+
33. Shen, H., Toki, H., Oyamatsu, K., Sumiyoshi, K.: Relativistic Equation of State of Nuclear Matter for Supernova Explosion. Progress of Theoretical Physics **100** (1998) 1013–1031
34. Hillebrandt, W., Wolff, R.G.: Models of Type II Supernova Explosions. In Arnett, W.D., Truran, J.W., eds.: Nucleosynthesis: Challenges and New Developments, Chicago, University of Chicago Press (1985) 131
35. Marek, A.: The effects of the nuclear equation of state on stellar core collapse and supernova evolution. Diplomarbeit, Technische Universität München (2003)
36. Mihalas, D., Weibel Mihalas, B.: Foundations of Radiation Hydrodynamics. Oxford University Press, Oxford (1984)